Published OnlineFirst February 1, 2017; DOI: 10.1158/1541-7786.MCR-16-0322

Chromatin, Epigenetics, and RNA Regulation

Molecular Cancer Research

Prognostic Relevance of Tumor Purity and Interaction with MGMT Methylation in Glioblastoma

Eva Schulze Heuling[1], Felix Knab[1], Josefine Radke[2,3,4], Eskil Eskilsson[5], Emmanuel Martinez-Ledesma[5], Arend Koch[2], Marcus Czabanka[6], Christoph Dieterich[7], Roel G. Verhaak[5,8], Christoph Harms[1,4,9], and Philipp Euskirchen[1,4,10]

Abstract

Promoter methylation status of O-6-methylguanine-DNA methyltransferase (MGMT), a DNA repair enzyme, is a critical biomarker in glioblastoma (GBM), as treatment decisions and clinical trial inclusion rely on its accurate assessment. However, interpretation of results is complicated by poor interassay reproducibility as well as a weak correlation between methylation status and expression levels of MGMT. This study systematically investigates the influence of tumor purity on tissue subjected to MGMT analysis. A quantitative, allele-specific real-time PCR (qAS-PCR) assay was developed to determine genotype and mutant allele frequency of telomerase promoter (pTERT) mutations as a direct measure of tumor purity. We studied tumor purity, pTERT mutation by Sanger sequencing, MGMT methylation by pyrosequencing, IDH1 mutation status, and clinical parameters in a cohort of high-grade gliomas ($n = 97$). The qAS-PCR reliably predicted pTERT genotype and tumor purity compared with independent methods. Tumor purity positively and significantly correlated with the extent of methylation in MGMT methylated GBMs. Extent of MGMT methylation differed significantly with respect to pTERT mutation hotspot (C228T vs. C250T). Interestingly, frontal lobe tumors showed greater tumor purity than those in other locations. Above all, tumor purity was identified as an independent prognostic factor in GBM. In conclusion, we determined mutual associations of tumor purity with MGMT methylation and pTERT mutations and found that the extent of MGMT methylation reflects tumor purity. In turn, tumor purity is prognostic in IDH1 wild-type GBM.

Implications: Tumor purity is an independent prognostic marker in glioblastoma and is associated with the extent of MGMT methylation. *Mol Cancer Res; 15(5); 532–40. ©2017 AACR.*

Introduction

O-6-Methylguanine-DNA methyltransferase (MGMT) promoter methylation is currently the most important biomarker in glioblastoma (GBM), as it informs treatment options and is used as an inclusion criterion in clinical trials. Quantitative assays (such as bisulfite pyrosequencing) use a defined threshold to identify methylated cases. Yet, the high variability of the extent of MGMT promoter methylation (i.e., the percentage of methylated alleles) has generated debate regarding its origin. Sources of intratumoral heterogeneity may include phenotypic plasticity of tumor cells (such as cancer stem cells vs. non-stem cells) and tumor purity (caused by sampling bias or immune infiltration). Importantly, a prognostic value is suggested not only for a dichotomous MGMT promoter methylation status but also for the extent of methylation (1). It is therefore critical to standardize tumor purity of the input material for reproducible results (2). However, systematic investigation of tumor purity has been hindered by the lack of scalable assays. Here, we use a novel tumor purity assay to investigate the correlation between tumor purity and MGMT methylation.

Defining tumor purity

Cancer, although etiologically a disease of the genome, involves a complex ecosystem of stromal and immune cell populations interacting with and sometimes supporting tumor cells. Accordingly, solid tumors are cellularly heterogeneous. Compared with grade 2 and grade 3 astrocytomas, immune infiltration [mainly by microglia and tumor-associated macrophages (TAM)] is a hallmark of GBM, which is the most frequently occurring

[1]Department of Experimental Neurology, Charité – Universitätsmedizin Berlin, Berlin, Germany. [2]Department of Neuropathology, Charité – Universitätsmedizin Berlin, Berlin, Germany. [3]German Consortium for Translational Cancer Research (DKTK), Heidelberg, Germany. [4]Berlin Institute of Health (BIH), Berlin, Germany. [5]Department of Genomic Medicine, University of Texas MD Anderson Cancer Center, Houston, Texas. [6]Department of Neurosurgery, Charité – Universitätsmedizin Berlin, Berlin, Germany. [7]Computational RNA Biology and Ageing Group, Max-Planck-Institute for the Biology of Ageing, Cologne, Germany. [8]Department of Bioinformatics and Computational Biology, University of Texas MD Anderson Cancer Center, Houston, Texas. [9]Center for Stroke Research Berlin, Charité – Universitätsmedizin Berlin, Berlin, Germany. [10]Department of Neurology, Charité – Universitätsmedizin Berlin, Berlin, Germany.

Note: Supplementary data for this article are available at Molecular Cancer Research Online (http://mcr.aacrjournals.org/).

Corresponding Authors: Philipp Euskirchen, Charité – Universitätsmedizin Berlin, Charitéplatz 1, Berlin 10117, Germany. Phone: 49-30-450-560635; Fax: 49-30-450-560930; E-mail: philipp.euskirchen@charite.de; and Christoph Harms, christoph.harms@charite.de

doi: 10.1158/1541-7786.MCR-16-0322

Published OnlineFirst February 1, 2017; DOI: 10.1158/1541-7786.MCR-16-0322

primary malignant brain tumor in adults. This poses the theoretical and practical challenge to unequivocally delineate putative tumor cells (defined as the progeny of a genetically distinct most recent common ancestor cell) from normal or reactive cells in the tumor microenvironment. Distinction has historically been made histologically by morphologic features, such as nuclear atypia. However, a systematic pan-cancer comparison found poor correlation of a hematoxylin–eosin (H&E) stain–based tumor purity measure with gold standard genome-wide approaches (3).

With the advent of next-generation sequencing technologies, a map of the landscape of structural genetic alterations, mutated genes, and signaling pathways has been sketched to facilitate identification of driver mutations on a population level. Meanwhile, within an individual tumor, it remains challenging to identify the defining features of a most recent common ancestor. Current tumor purity assays rely on whole-genome, exome, or transcriptome data that are complex and expensive.

Noncoding mutations in the telomerase promoter (pTERT) region have recently been identified with high prevalence in solid tumors, especially GBM (4–10). Importantly, they have been shown to be clonal mutations in gliomas (11) and are likely to play a role in tumor initiation (12). Using clonal pTERT mutations as the defining characteristic of a GBM tumor cell, we established a convenient PCR-based assay to systematically study clinical and molecular consequences of varying tumor purity.

Materials and Methods

Cell lines and patient samples

The generation of primary glioma cell lines was approved by the local ethics committee (Charité – Universitätsmedizin Berlin, Berlin, Germany; EA1/265/12). The study has been registered in compliance with ICMJE guidelines (German Clinical Trials Register ID: DRKS00004577, UTN trial number: U1111-1137-4400). Surgical and blood samples were deposited after written informed consent in the tumor and biobank at the Charité Comprehensive Cancer Center (Berlin, Germany). Glioma samples were divided immediately after surgical removal: For histology and nucleic acid extraction, specimens were snap frozen within one hour after surgery; for cell culture, specimens were kept sterile in Hank's Balanced Salt Solution (HBSS, Life Technologies) on ice until tissue dissociation.

Tumor specimens were first dissociated mechanically, washed in HBSS, and then digested enzymatically using Liberase DH (Roche) for 30 minutes at 37°C. The enzyme blend was inactivated by DMEM + 20% FCS. A single-cell suspension was prepared by gentle trituration and filtering the suspension through a 40-μm cell strainer (BD Biosciences). After washing in PBS, erythrocytes were lysed by incubation on ice with EasyLyse buffer (Dako) for 10 minutes. Cells were washed twice in PBS and resuspended in complete neural stem cell medium with growth factors. Glioma cell lines have been deposited at the German Collection of Microorganisms and Cell Cultures (Leibniz Institute, Braunschweig, Germany, http://www.dsmz.de). Cell lines were authenticated using SNP profiles generated from the same RNA sequencing (RNA-seq) data used for expression analysis and purity estimation.

Ninety-seven consecutive cases of high-grade gliomas diagnosed from 2014 to 2015, in which DNA samples [extracted from formalin-fixed paraffin-embedded (FFPE) tissue] had been subjected to clinical routine MGMT analysis, were selected retrospectively for study. All tissue samples had been macrodissected to select for viable tumor, aiming at >80% tumor nuclei as estimated visually in H&E stains where possible.

Cell culture

Cells were grown in Neurobasal Medium (Life Technologies) supplemented with 0.5× N2 supplement (Life Technologies) and 0.5× B27 (Life Technologies) as described previously (13), but with 20 ng/mL EGF (PeproTech), 20 ng/mL bFGF (PeproTech). Spheroids were dissociated using Accutase (Life Technologies). For cryopreservation, neurospheres were dissociated and resuspended in complete medium with 10% DMSO. The cell suspension was transferred to cryotubes and kept at −80 °C for 24 hours, then moved to liquid nitrogen tanks for long-term storage. For thawing, cells were quickly brought to room temperature. Cells were washed once in growth medium before being transferred to cell culture flasks.

Quantitative allele-specific real-time PCR

Real-time PCR was performed on a realplex epGradient S PCR cycler (Eppendorf). For a 20-μL reaction, 10 μL 2× QuantiTect SYBR Green Master Mix (Qiagen), 1 μL of a 10 μmol/L forward and reverse primer mix, and 1 μL template DNA (normalized to 25 ng/μL) were used. Fifty cycles of 15-second denaturation at 94°C, 30-second annealing and 30-second extension at 72°C were performed. Melting curve analysis was used to exclude primer–dimer formation and ensure proper amplification. Primers and annealing temperatures are listed in Supplementary Table S2. All reactions were performed in duplicates. For quantification, standard curves for each primer pair were generated using serial dilutions of a heterozygous DNA sample to determine absolute copies. Mutant allele frequency (MAF) was then calculated as follows:

$$\text{MAF} = \text{mutant copies}/(\text{wild-type copies} + \text{mutant copies})$$

The majority of GBM cases (81%) retain a diploid TERT locus as determined from GISTIC2 threshold copy number data in TCGA GBMs (data not shown). In addition, most pTERT mutations (190/197; 96% of cases in one study) are reported to be heterozygous (8). Thus, generally, tumor purity can be calculated as 2× MAF. However, we chose to report MAF instead of purity to avoid these assumptions. Where information about the homozygous versus heterozygous nature of the pTERT mutation was available from matched cell lines, actual tumor purity was calculated, taking into account zygosity.

Sanger sequencing

The pTERT region flanking the C228 and C250 loci was amplified from 50 ng genomic DNA using 1 U Phusion polymerase (Life Technologies), 0.5 μmol/L forward and reverse primers, 200 μmol/L dNTPs, 10 μL 5× HF buffer, and 5% DMSO in a total volume of 50 μL. The following primers were used: forward 5′-TGT AAA ACG ACG GCC AGT GGC CGA TTC GAC CTC TCT-3′, reverse 5′-AGC ACC TCG CGG TAG TGG-3′ (5). The PCR program consisted of 10-minute initial denaturation at 98°C, 40 cycles of 1-minute denaturation at 98°C, 30-second annealing at 65°C, and 30-second elongation at 72°C, followed by a final 10-minute elongation step. Sequencing was performed using a M13 universal primer (5′-TGT AAA ACG ACG GCC AGT-3′, Eurofins Genomics).

Base calls were made using R/Bioconductor and the sangerseqR package (14, 15) using a cut-off ratio of 0.33 for heterozygous

Published OnlineFirst February 1, 2017; DOI: 10.1158/1541-7786.MCR-16-0322

calls. Reads were then aligned to the hg19 reference genome assembly using bwa 0.7.8-r455 (16), and variants were called using samtools and bcftools 1.1 (17).

MGMT promoter methylation assay

Quantitative analysis of MGMT methylation was performed using bisulfite pyrosequencing. A total of 500 ng of genomic DNA was subjected to bisulfite conversion using the EZ DNA Methylation Kit (Zymo Research) according to the manufacturer's protocol. PCR amplicons covering five CpG islands in the MGMT locus (hg19 coordinates: chr10:131,265,507 - 534, CGCTTTGCGTCCCGACGCCCGCAGGTCC) were generated using commercially available primers (Qiagen; cat. number 972032) and subjected to pyrosequencing on an automated PyroMark Q24 System (Qiagen) following the manufacturer's instructions. Data were analyzed and quantified with the PyroMark Q24 Software 2.0 (Qiagen). The mean percentage of methylated alleles at all five loci was used for analysis. We defined a cutoff value of 10% to classify MGMT methylated versus nonmethylated cases, which is commonly used (18) and has been validated internally for routine clinical diagnostics.

RNA-seq

RNA was extracted from tumor tissue using the mirVana RNA Isolation Kit (Life Technologies) or using TRIzol (Life Technologies) and RNeasy columns (Qiagen) following the manufacturer's instructions. RNA quantity and quality were determined using a Bioanalyzer RNA Nano Assay (Agilent), and an RIN > 7.0 was required for use in sequencing. Poly(A)-enriched RNA-seq libraries were generated using NEXTflex RNA-Seq Kits and Barcodes (Bioo Scientific) and sequenced on a HiSeq instrument (Illumina). Sequence data have been deposited at the European Genome-phenome Archive (EGA, http://www.ebi.ac.uk/ega) under accession number EGAD00001002893. For expression analysis, reads were aligned to the hg38 reference genome using STAR aligner 2.4.1d (19) and gene-level expression values were generated and normalized for library size using cufflinks (20).

Tumor purity estimation from RNA-seq data

RNA-seq raw data were reprocessed using PRADA (21) after removal of unpaired reads. Transcripts were filtered for size and protein-coding genes. Expression data normalized to reads per kilobase per million reads (RPKM) were then subjected to the ESTIMATE algorithm to deconvolute bulk tumor gene expression profiles with respect to stromal and immune cell infiltration and derive an estimate of tumor purity as described before (22).

Public datasets

Survival data, MGMT, and IDH1 status for the 2013 glioblastoma cohort of The Cancer Genome Atlas (TCGA) were retrieved from the supplementary data of the lead publication (23). Preprocessed Affymetrix platform gene expression data (compiled August 8, 2014) were downloaded from the UCSC Cancer Genome Browser (24). Tumor purity was calculated using the R implementation of the ESTIMATE algorithm (version 1.0.11). The subset of 275 IDH wild-type cases with complete information on survival, tumor purity, MGMT status, and age was used for all subsequent analyses.

Results

A mutation-specific telomerase promoter PCR quantifies tumor purity

Although allele-specific PCR has been used qualitatively for genotyping glioma (25), it can also be performed quantitatively for allele frequency estimation (26). To sensitively detect telomerase promoter mutations, we established an allele-specific quantitative real-time PCR (qAS-PCR) assay for the two commonly observed hotspot mutations (chr5:1,295,228G>A and chr5:1,295,250G>A) in the TERT promoter (Fig. 1A), which is able to discriminate mutant and wild-type alleles (Fig. 1B and C). In a panel of 13 human GBM and 9 matched GBM stem cell lines, qAS-PCR and Sanger sequencing identified identical pTERT genotypes for all cell lines and parental tumors for which data from both methods were available (Supplementary Table S1).

Quantitative interpretation of AS-PCRs for both wild-type and mutated alleles enables determination of the MAF (26). Based upon MAF, we estimated the percentage of cells carrying a pTERT mutation (i.e., tumor purity).

We validated the linearity of the assay using serial dilutions of mutant and wild-type DNA at defined ratios (Fig. 1D and E). Both the C228T assay (Pearson $r = 0.92$, $P < 10^{-7}$) and the C250T assay (Pearson $r = 0.996$, $P < 10^{-11}$) showed strong correlation between theoretical and observed MAF.

Notably, we also evaluated primers with a locked nucleic acid modified 3′ base to improve discrimination (27, 28). Although this greatly improved specificity for qualitative applications (i.e., genotyping), it reduced the dynamic performance of the assay with poor linearity (data not shown). Accordingly, we selected conventional primers for all subsequent experiments.

To cross-validate pTERT MAF-derived tumor purity using an independent method, we used deconvolution of gene expression profiles using the ESTIMATE algorithm (22). In the panel of GBMs used for cell line generation, DNA for pTERT qAS-PCR and RNA for RNA-seq and subsequent deconvolution were extracted from adjacent fresh tissue sections for parental tumors or similar passages in case of cell lines, respectively (total number of matched DNA/RNA pairs: $n = 17$). The use of cell lines enabled unequivocal discrimination of heterozygous versus homozygous mutations, which was taken into account for tumor purity calculation. We observed a robust positive correlation between the two orthogonal methods with both the C228T (Spearman $\rho = 0.68$, $P = 0.01$) and C250T (Spearman $\rho = 0.88$, $P = 0.02$) assay, respectively (Fig. 1F and G). In addition, both methods sufficiently discriminated bulk tumor tissue from their matched cell line by identifying greater tumor purity in cell lines (pTERT qAS-PCR 5/6, ESTIMATE 6/6; Supplementary Fig. S1).

pTERT qAS-PCR enables genotyping of clinical routine samples

We next selected 97 consecutive cases of high-grade gliomas from 2014 to 2015 in which clinical routine DNA samples (extracted from FFPE tissue after macrodissection of viable tumor tissue) were subjected to MGMT analysis. Histologic diagnosis was GBM in 78% (76/97) of cases, 4% (4/97) were anaplastic oligodendroglioma, 8% (8/97) anaplastic astrocytoma, 5% (5/97) anaplastic oligoastrocytoma, and 2% (2/97) gliosarcoma. Two cases with final diagnosis of primitive neuroectodermal tumor and pilocytic astrocytoma, respectively, were excluded from analysis. MGMT methylation status was determined by

Published OnlineFirst February 1, 2017; DOI: 10.1158/1541-7786.MCR-16-0322

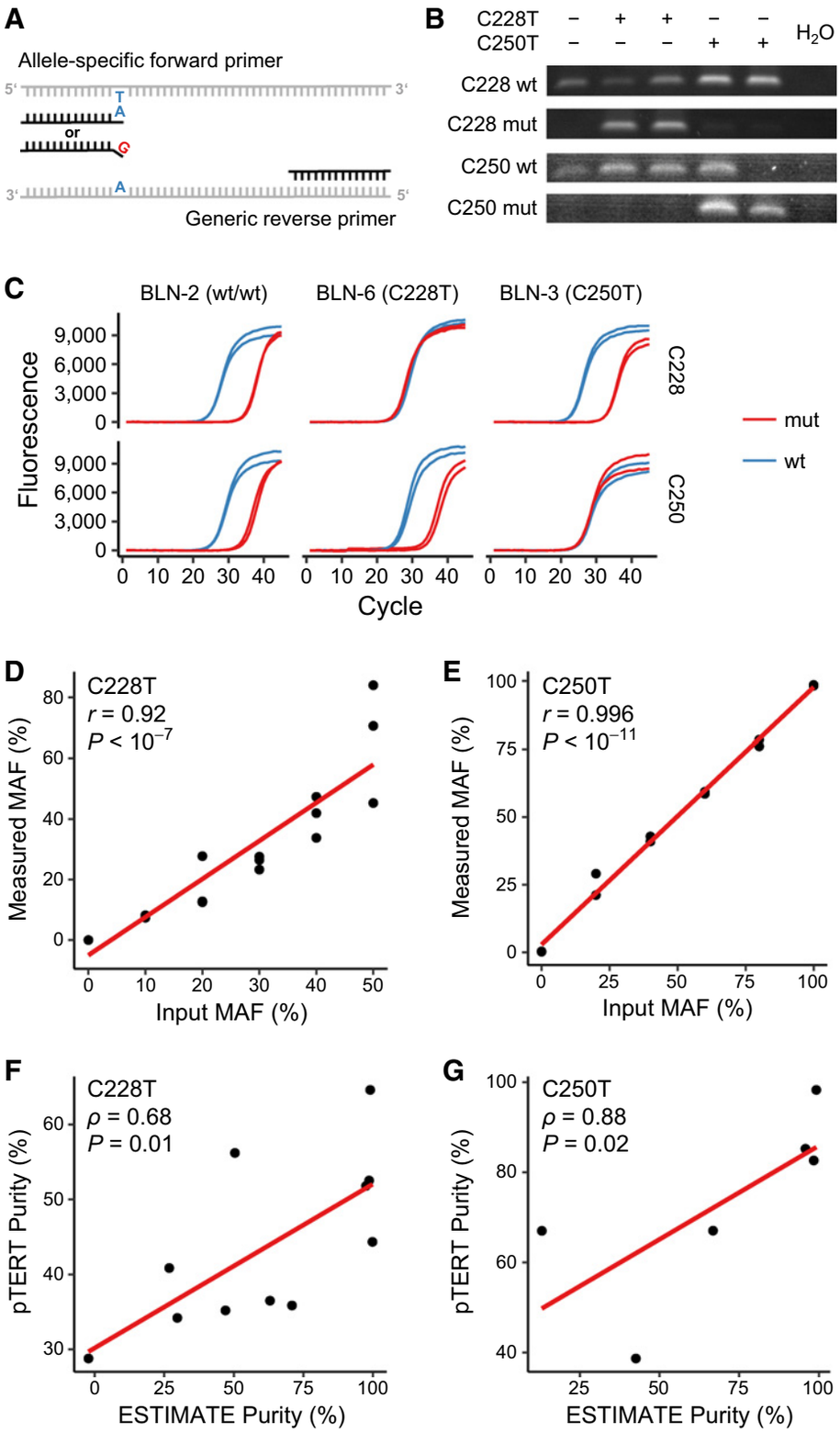

Figure 1.

qAS-PCR of pTERT mutations quantifies tumor purity. **A,** Schematic illustration of AS-PCR. Allele-specific primers discriminate single nucleotide differences to quantify the abundance of wild-type versus mutant alleles. **B,** Example gel electrophoresis of PCR products generated by AS-PCR from GBM cell lines with different pTERT genotypes. Note the missing wild-type band in a homozygously C250T mutated sample (lane 5). A no-template reaction is run along as negative control. **C,** Amplification curves for C228 and C250 quantitative AS-PCR illustrate the discrimination of wild-type and mutant alleles in GBM cell lines. The ratio between amplification of the targeted versus nontargeted is approximately 1,000-fold (~10 cycles). **D** and **E,** Validation of assay linearity using artificial mixtures of mutant and wild-type DNA. **F** and **G,** Orthogonal validation of qAS-PCR by deconvolution of bulk gene expression profiles.

pyrosequencing, IDH1 mutation status by IHC or sequencing was available for 93 of 97 cases, and telomerase promoter mutations were identified by Sanger sequencing for 88 of 97 cases. In GBM, a mutually exclusive pattern of pTERT mutations and IDH mutations was observed (Fig. 2A). The frequency of pTERT mutations in GBM was 77.1% (54/70 cases, 95% confidence interval,

Published OnlineFirst February 1, 2017; DOI: 10.1158/1541-7786.MCR-16-0322

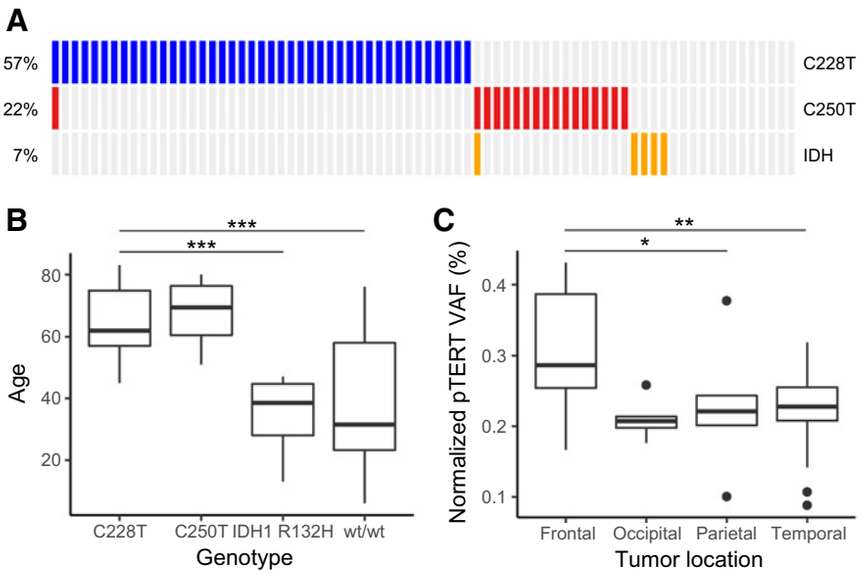

Figure 2.
Molecular and clinical characteristics of glioblastoma cases. **A,** Mutual exclusivity of pTERT hotspot and IDH1 mutations in GBM. Percentages indicate the prevalence of the corresponding alteration in the GBM subset of the cohort ($n = 76$). **B,** Age differences in GBM patients with respect to pTERT and IDH1 genotype. **C,** Tumor purity with respect to neuroanatomical location. Cases with ambiguous clinical information regarding the affected lobe (e.g., parieto-occipital) were excluded. Boxplots show group median (thick lines), quartile range (boxes), 1.5× interquartile range (whiskers), and outlier samples (dots). Asterisks indicate significant group differences as determined by linear regression (*, $P < 0.05$; **, $P < 0.01$; ***, $P < 0.001$).

67.3–86.9), which is comparable with published prevalences (5–7). One case carried both pTERT hotspot mutations as determined by both Sanger sequencing and qAS-PCR. Notably, GBM patients with wild-type pTERT and wild-type IDH1 significantly differed with respect to age (Fig. 2B). A single-nucleotide variant (SNP) in the TERT promoter region known to disrupt an ETS transcription factor–binding motif, rs2853669, was assessed in 96 of 100 samples.

We also determined pTERT genotypes using qAS-PCR. qAS-PCR called identical pTERT hotspot mutations in 86 of those 88 cases (98%) where Sanger sequencing data of the telomerase promoter region were available as well.

Extent of MGMT hypermethylation reflects tumor purity

We investigated relationships between MGMT promoter methylation and tumor purity (Fig. 3). In all analyses, we used quantile-normalized pTERT-MAF as tumor purity measure. Mean tumor purity did not differ between MGMT methylated (pTERT MAF 0.26 ± 0.06) and unmethylated (0.26 ± 0.08) cases.

Importantly, we found a robust positive correlation between tumor purity and extent of MGMT methylation (Spearman $\rho = 0.45$, $P = 0.006$) in MGMT methylated tumors (Fig. 3B). The effect was even more pronounced when restricting the correlation to GBM samples (Spearman $\rho = 0.50$, $P = 0.008$). No significant correlation was observed for cases classified as MGMT unmethylated.

Tumor purity itself is prognostic for overall survival

Extent of MGMT methylation has previously been reported to predict survival in patients receiving temozolomide (1). Given the strong association between tumor purity and the extent of MGMT methylation, we investigated the effect of tumor purity itself on overall survival in IDH1 wild-type GBM cases from TCGA (23). Tumor purities for TCGA GBMs were determined using ESTIMATE (22). For MGMT status, we used methylation calls from the original publication using the STP27 model from microarray-based methylation data (29). In univariate analysis, tumor purity was a significant positive predictor (HR = 0.30, $P = 0.012$) of overall survival (Table 1). MGMT status and age, both of which are known prognostic factors, also had significant impact in univariate analysis. In multivariate analysis, however, only tumor purity (HR = 0.28, $P = 0.011$) and age (HR = 1.04, $P < 10^{-8}$) emerged as independent prognostic factors (Table 1). TCGA data thus suggest that high purity confers a more favorable overall survival.

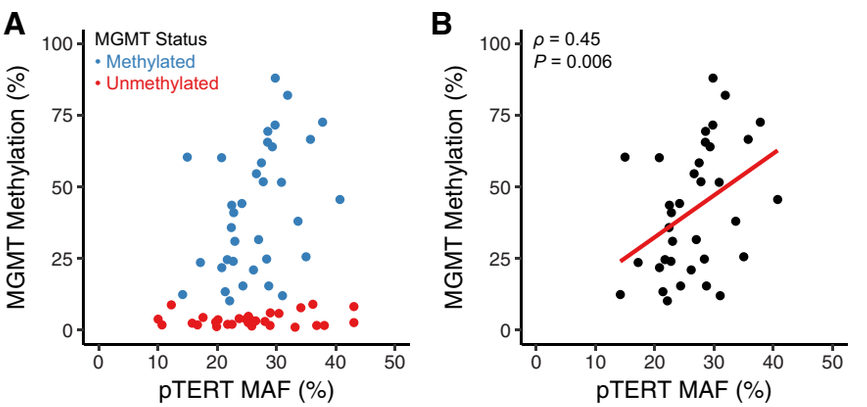

Figure 3.
Correlation of tumor purity and extent of MGMT methylation. **A,** Scatter plot of pTERT MAF as a direct measure of tumor purity versus mean MGMT methylated allele frequency across five CpG islands per tumor in pTERT mutant gliomas ($n = 65$). **B,** Correlation of pTERT-MAF and mean MGMT methylated allele frequency in MGMT methylation positive gliomas ($n = 35$) using Spearman ρ.

Published OnlineFirst February 1, 2017; DOI: 10.1158/1541-7786.MCR-16-0322

Table 1. Overall survival analysis in TCGA glioblastoma cohort

	Univariate analysis ($n = 275$)		Multivariate analysis ($n = 275$)	
Factor	**HR (95% CI)**	**Significance level**	**HR (95% CI)**	**Significance level**
ESTIMATE tumor purity (continuous)	0.30 (0.12–0.76)	$\mathbf{P = 0.012}$	0.28 (0.10–0.75)	$\mathbf{P = 0.011}$
MGMT status (methylated vs. unmethylated)	0.74 (0.56–0.99)	$\mathbf{P = 0.043}$	0.78 (0.58–1.04)	$P = 0.088$
Age (years)	1.04 (1.03–1.05)	$\mathbf{P < 10^{-9}}$	1.04 (1.03–1.05)	$\mathbf{P < 10^{-8}}$

NOTE: Information on overall survival, tumor purity, MGMT status, and age was available for $n = 275$ IDH1 wild-type cases from the 2013 TCGA GBM cohort. A Cox proportional hazards model was fit for both univariate and multivariate analysis. Tumor purity was computed from cDNA microarray gene expression data using ESTIMATE. Bold font indicates a significance level of $P < 0.05$.
Abbreviation: 95% CI, 95% confidence interval.

MGMT methylation varies across pTERT genotypes

Next, we correlated MGMT methylation with genotypes for pTERT and IDH1. The frequency of MGMT methylated cases was not significantly different between genotypes both for all tumor entities (Fisher exact test, $P = 0.08$, Fig. 4C) and GBM only ($P = 0.53$, Fig. 4D). The extent of methylated alleles, however, differed significantly between C228T and C250T pTERT mutations for pooled entities (linear regression model, $P = 0.004$, Fig. 4A) and GBM alone ($P = 0.046$, Fig. 4B).

TERT expression and MGMT methylation

Distinct levels of transcriptional activity have been attributed to different pTERT mutations (30). We therefore compared levels of *TERT* mRNA expression in GBM cell lines and their matched parental tumors. Although nonsignificant and subject to careful interpretation given the low sample numbers, higher telomerase levels were found in cell lines with C228T versus C250T mutations as described before (Fig. 5A). In contrast, *TERT* expression in bulk tumor material with varying degrees of tumor purity showed higher levels in C250T-mutated tumors (Fig. 5B). We then correlated *TERT* mRNA expression with levels of MGMT methylation. No significant correlation (Pearson $r = -0.53$, $P = 0.22$) was present in cell lines (Fig. 5C), but a positive correlation (Pearson $r = 0.88$, $P = 0.0016$) was found in pTERT-mutant tumors (Fig. 5D), possibly a spurious relationship due to collinearity of both factors with tumor purity.

Regional differences in tumor purity

We explored differences in tumor purity with respect to tumor location. Clinical annotation that allowed unequivocal attribution of tumor location to a single brain lobe and tumor purity information was available for 40 of 59 pTERT-mutant GBM cases. Frontal lobe tumors revealed significantly greater tumor purity compared with temporal lobe (pTERT-MAF 0.3 ± 0.09 vs. 0.22 ± 0.1; $P < 0.01$) and occipital lobe (0.3 ± 0.09 vs. 0.21 ± 0.03; $P = 0.027$) locations (Fig. 2C).

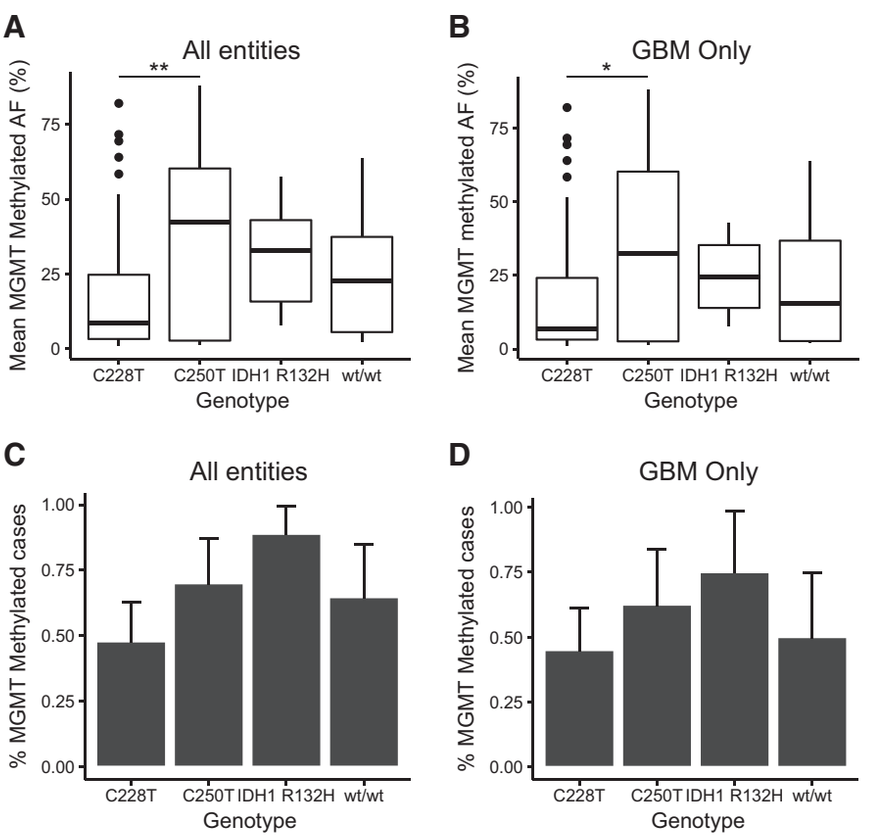

Figure 4.
Differences in MGMT methylation with respect to pTERT and IDH status. **A** and **B,** Aggregated mean MGMT methylated allele frequency (AF) across pTERT and IDH1 mutation status. **C** and **D,** Frequency of MGMT methylated cases across pTERT and IDH1 mutation status. Error bars, 95% confidence intervals. Either all high-grade gliomas (**A** and **C**) or GBM cases only (**B** and **D**) are shown. Cases with concurrent C228T and C250T mutation or pTERT and IDH1 mutation, respectively, were excluded. Asterisks indicate significant group differences as determined by linear regression (*, $P < 0.05$; **, $P < 0.01$).

Published OnlineFirst February 1, 2017; DOI: 10.1158/1541-7786.MCR-16-0322

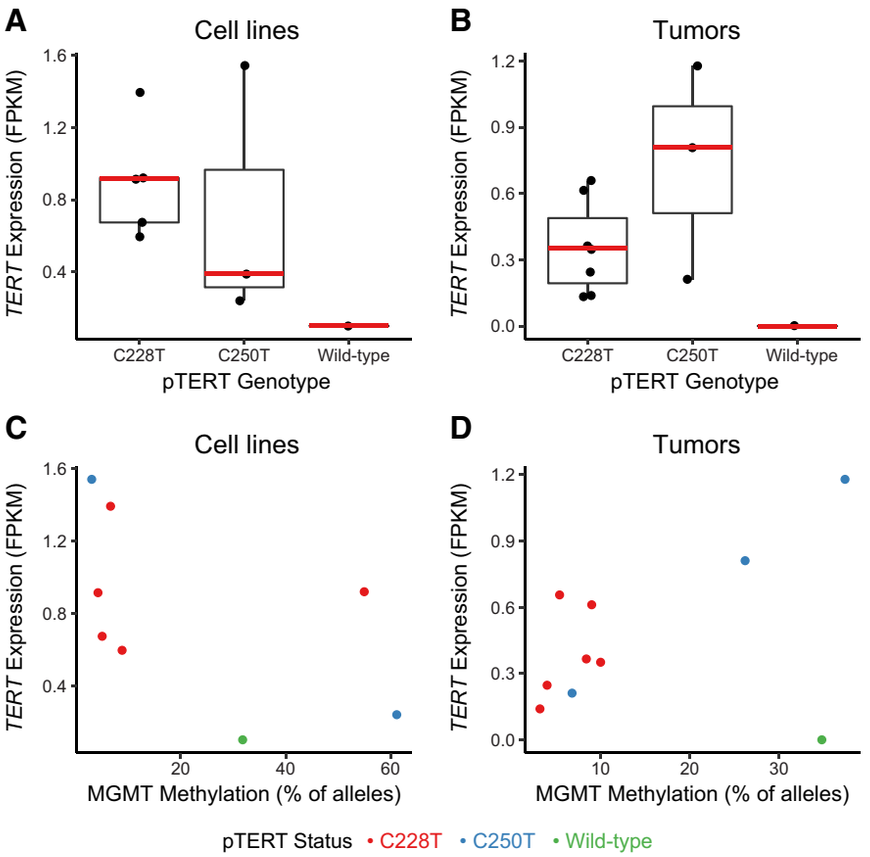

Figure 5.
Telomerase expression with respect to pTERT genotype and MGMT methylation. *TERT* mRNA expression levels in a panel of matched GBM cell lines and parental tumors (Supplementary Table S1) as determined by RNA-seq (fragments per kilobase of exon per million reads, FPKM). **A** and **B,** Boxplots show expression levels for each pTERT genotype (group median indicated in red). **C** and **D,** Correlation between MGMT methylated allele frequency (%) and *TERT* expression. Pearson product–moment correlation coefficients were calculated for the subset of pTERT-mutant samples only.

Technical considerations

Finally, we pondered whether or not low tumor purity limits the sensitivity of clinical routine molecular diagnostics and perhaps generates false-negative results. Accordingly, we investigated whether or not MGMT methylated cases occurred more frequently in samples with high purity, which would implicate tumor purity as a confounder of assay sensitivity. No significant differences could be identified using a logistic regression model (MGMT status $\sim$ pTERT-MAF, $P > 0.05$).

We also examined MGMT methylation of matched tumor and cell lines in the BLN panel. In 7 of 8 cases, MGMT status was identical between pairs. In the discordant sample pair (BLN-11), the parental tumor was classified negative using the clinical routine threshold of 10% for MGMT pyrosequencing, while the corresponding cell line showed clearly positive MGMT methylation (Supplementary Table S1). Tumor purity was comparably low in this sample (ESTIMATE 36th percentile, C228T MAF 29th percentile). In summary, low tumor purity might generate false-negative results in exceptional cases.

Discussion

Using a novel tumor purity assay, we identified clinically relevant associations between tumor purity, pTERT hotspot mutations, and MGMT methylation.

We first identified tumor purity as a relevant contributor to the observed variability of the extent of MGMT promoter methylation reported by all quantitative methods. This finding is supported by a series of 10 tumors and matched gliomasphere cell lines, which revealed concordant MGMT methylation status with increased methylated allele frequency in 9 of 10 pairs (31). Extent of methylation differed especially in tumor samples with infiltration by $CD68^+$ cells (i.e., macrophages and microglia). Although tumor purity is recognized as a critical confounder when distinguishing nonmethylated versus methylated tumors (2), the source of variability in distinctly positive samples has been a matter of debate. Importantly, the extent of MGMT methylation has itself been reported to have prognostic value. Using pyrosequencing, Dunn and colleagues found a survival advantage of highly methylated tumors in a cohort of 109 patients homogeneously treated with temozolomide and standard radiotherapy (1). Similarly, another study reported an intermediate overall survival for patients with tumors producing a faint band in methylation-specific PCR compared with both unmethylated and distinctly methylated cases (32). Our analysis of TCGA data suggests that tumor purity is a predictor of survival, raising the question of which biological mechanism is responsible for this phenomenon.

Tumor purity is a reciprocal measure of the contribution of cellular microenvironment components, namely immune cells, endothelial cells, and normal brain tissue. As the largest contribution likely arises from tumor-associated microglia and macrophages, perhaps there is a negative prognostic influence of immune cell infiltration that is supported by a large body of preclinical evidence suggesting that TAMs support tumor growth in glioma (33). Angiogenesis, yielding increased numbers of endothelial cells

and possibly pericytes, might also contribute negatively to tumor purity; however, whether or not they alter tumor purity in a relevant manner has not been studied quantitatively.

Heterogeneity of MGMT methylation within the tumor cell population has been reported as another source of variability of MGMT promoter methylation. One study observed the presence of both methylated and unmethylated clones in gliomaspheres derived from single cells of the same parental tumor by analyzing both protein expression and promoter methylation (34). Notably, neither MGMT methylation nor protein expression correlated with temozolomide resistance in this study.

Temporal heterogeneity of MGMT methylation is conceivable; however, matched primary GBM and their recurrences have largely revealed identical MGMT status, and retesting is currently discouraged in clinical guidelines (35). Loss of chromosome 10q has also been considered a factor influencing MGMT methylation, but recent studies found no correlation between MGMT copy number and extent of methylation in GBM (32) or low-grade gliomas (36).

In summary, tumor purity explains part of the variability observed in the levels of MGMT methylation. We can only speculate about the biological causes of tumor purity that explain its prognostic significance, especially the role of immune cells. From a clinical perspective, it would be interesting to investigate whether tumor purity differentially predicts response to chemotherapy versus radiation and whether modulation of the tumor microenvironment is by treatment is reflected in tumor purity.

We also identified differences in the extent of MGMT methylation between pTERT hotspot mutations. The frequency of MGMT methylation was not statistically different, although we are mindful that the study was underpowered with respect to the observed group differences. To our knowledge, all studies of pTERT mutations in GBM to date do not differentiate MGMT status between the two exact point mutations. For example, although Simon and colleagues found no differences in frequency of MGMT methylation between pTERT mutant and wild-type tumors, the researchers did not differentiate between C228T and C250T mutations (9).

This is perhaps reasonable as both hotspot mutations are known to generate an identical Ets/TCF transcription factor–binding motif (37–39). Very recently, however, functional differences between the C228T and C250T mutations with respect to NF-κB pathway activation has been reported (40). Profound biological differences, for example, in tumor purity, between tumors carrying the C228T versus the C250T point mutation are thus likely. We were unable to test whether or not the observed differences in the extent of MGMT methylation actually reflect differences in tumor purity because of the required quantile normalization between the C228 and C250 qAS-PCR assays. Similarly, several studies have shown differences in *TERT* mRNA expression levels between the two hotspot mutations with higher expression in C250T-mutated GBM samples (23, 40). We observed the same trend in our data, but we instead propose attributing this finding to collinearity with tumor purity. At the same time, an exogenous C228T mutation previously showed higher promoter activity in a luciferase reporter assay (30), a finding that we recapitulated in glioma cell lines where tumor purity does not confound readouts. Taken together, we propose that on the bulk tumor level, it is most likely tumor purity that explains best variability in telomerase expression in pTERT-mutant GBM, while distinct pTERT mutations dictate different promoter activity.

Finally, we report tumor purity differences with respect to tumor location. Frontal lobe tumors show substantially greater tumor content than all other locations. Whether or not this is due to a heterogeneous cellular composition with respect to immune infiltration, angiogenesis, resident glial architecture, or even a systematic sampling bias caused by surgical accessibility remains a matter of speculation.

It is important to note that all analyses involving pTERT MAF–based tumor purity were restricted to pTERT-mutated cases, so we cannot exclude a selection bias (largely IDH mutant and pTERT/IDH double wild-type cases). In addition, absolute quantification of tumor purity, while feasible using qAS-PCR, will require further optimization of the method to circumvent cross-assay normalization.

In conclusion, we describe a convenient assay for the systematic investigation of tumor purity in GBM as a tool for studying cellular composition and quality control in molecular diagnostics. We report clinically relevant mutual associations between tumor purity, MGMT methylation status, and pTERT mutations. Although beyond the scope of the current study, investigation of the underlying biological causes is warranted. With respect to prognosis, we argue for a qualitative readout of MGMT methylation and prospective evaluation of tumor purity as an independent predictor of survival.

Disclosure of Potential Conflicts of Interest

No potential conflicts of interest were disclosed.

Authors' Contributions

Conception and design: E.S. Heuling, A. Koch, C. Harms, P. Euskirchen
Development of methodology: F. Knab, P. Euskirchen
Acquisition of data (provided animals, acquired and managed patients, provided facilities, etc.): E.S. Heuling, F. Knab, J. Radke, M. Czabanka, C. Dieterich, R.G. Verhaak, P. Euskirchen
Analysis and interpretation of data (e.g., statistical analysis, biostatistics, computational analysis): E.S. Heuling, J. Radke, E. Eskilsson, E. Martinez-Ledesma, A. Koch, C. Dieterich, P. Euskirchen
Writing, review, and/or revision of the manuscript: E.S. Heuling, F. Knab, J. Radke, E. Eskilsson, M. Czabanka, C. Harms, P. Euskirchen
Administrative, technical, or material support (i.e., reporting or organizing data, constructing databases): A. Koch
Study supervision: C. Harms, P. Euskirchen

Acknowledgments

The authors would like to acknowledge Randi Koll for expert technical assistance and Miriam Feldkamp and Janine Altmüller for RNA sequencing. The results published here are in part based upon data generated by The Cancer Genome Atlas (TCGA) project established by the NCI and NHGRI. Information about TCGA and the investigators and institutions who constitute the TCGA research network can be found at http://cancergenome.nih.gov/.

Grant Support

This work was supported by Berliner Krebsgesellschaft (EUFF-2012-36; to P. Euskirchen and C. Harms), the Einstein Foundation Berlin (EZK-2012-157; to P. Euskirchen), and the Berlin Institute of Health (TRG7, TP1; to C. Harms). J. Radke is a participant in the BIH-Charité Clinical Scientist Program funded by the Charité - Universitätsmedizin Berlin and the Berlin Institute of Health.

The costs of publication of this article were defrayed in part by the payment of page charges. This article must therefore be hereby marked *advertisement* in accordance with 18 U.S.C. Section 1734 solely to indicate this fact.

Received September 23, 2016; revised October 31, 2016; accepted January 24, 2017; published OnlineFirst February 1, 2017.

References

1. Dunn J, Baborie A, Alam F, Joyce K, Moxham M, Sibson R, et al. Extent of MGMT promoter methylation correlates with outcome in glioblastomas given temozolomide and radiotherapy. Br J Cancer 2009;101:124–31.
2. Wick W, Weller M, van den Bent M, Sanson M, Weiler M, von Deimling A, et al. MGMT testing—the challenges for biomarker-based glioma treatment. Nat Rev Neurol 2014;10:372–85.
3. Aran D, Sirota M, Butte AJ. Systematic pan-cancer analysis of tumour purity. Nat Commun 2015;6:8971.
4. Heidenreich B, Rachakonda PS, Hosen I, Volz F, Hemminki K, Weyerbrock A, et al. TERT promoter mutations and telomere length in adult malignant gliomas and recurrences. Oncotarget 2015;6:10617–33.
5. Killela PJ, Reitman ZJ, Jiao Y, Bettegowda C, Agrawal N, Diaz LA, et al. TERT promoter mutations occur frequently in gliomas and a subset of tumors derived from cells with low rates of self-renewal. Proc Natl Acad Sci U S A 2013;110:6021–6.
6. Koelsche C, Sahm F, Capper D, Reuss D, Sturm D, Jones DTW, et al. Distribution of TERT promoter mutations in pediatric and adult tumors of the nervous system. Acta Neuropathol 2013;126:907–15.
7. Labussière M, Boisselier B, Mokhtari K, Di Stefano AL, Rahimian A, Rossetto M, et al. Combined analysis of TERT, EGFR, and IDH status defines distinct prognostic glioblastoma classes. Neurology 2014;83:1200–6.
8. Nonoguchi N, Ohta T, Oh J-E, Kim Y-H, Kleihues P, Ohgaki H. TERT promoter mutations in primary and secondary glioblastomas. Acta Neuropathol 2013;126:931–7.
9. Simon M, Hosen I, Gousias K, Rachakonda S, Heidenreich B, Gessi M, et al. TERT promoter mutations: a novel independent prognostic factor in primary glioblastomas. Neuro Oncol 2015;17:45–52.
10. Spiegl-Kreinecker S, Lötsch D, Ghanim B, Pirker C, Mohr T, Laaber M, et al. Prognostic quality of activating TERT promoter mutations in glioblastoma: interaction with the rs2853669 polymorphism and patient age at diagnosis. Neuro Oncol 2015;17:1231–40.
11. Suzuki H, Aoki K, Chiba K, Sato Y, Shiozawa Y, Shiraishi Y, et al. Mutational landscape and clonal architecture in grade II and III gliomas. Nat Genet 2015;47:458–68.
12. Ceccarelli M, Barthel FP, Malta TM, Sabedot TS, Salama SR, Murray BA, et al. Molecular profiling reveals biologically discrete subsets and pathways of progression in diffuse glioma. Cell 2016;164:550–63.
13. Lee J, Kotliarova S, Kotliarov Y, Li A, Su Q, Donin NM, et al. Tumor stem cells derived from glioblastomas cultured in bFGF and EGF more closely mirror the phenotype and genotype of primary tumors than do serum-cultured cell lines. Cancer Cell 2006;9:391–403.
14. Hill JT, Demarest BL, Bisgrove BW, Su Y-C, Smith M, Yost HJ. Poly peak parser: method and software for identification of unknown indels using sanger sequencing of polymerase chain reaction products. Dev Dyn 2014;243:1632–6.
15. Huber W, Carey VJ, Gentleman R, Anders S, Carlson M, Carvalho BS, et al. Orchestrating high-throughput genomic analysis with Bioconductor. Nat Methods 2015;12:115–21.
16. Li H, Durbin R. Fast and accurate short read alignment with Burrows-Wheeler transform. Bioinformatics 2009;25:1754–60.
17. Li H, Handsaker B, Wysoker A, Fennell T, Ruan J, Homer N, et al. The Sequence Alignment/Map format and SAMtools. Bioinformatics 2009;25:2078–9.
18. Bienkowski M, Berghoff AS, Marosi C, Wöhrer A, Heinzl H, Hainfellner JA, et al. Clinical neuropathology practice guide 5-2015: MGMT methylation pyrosequencing in glioblastoma: unresolved issues and open questions. Clin Neuropathol 2015;34:250–7.
19. Dobin A, Davis CA, Schlesinger F, Drenkow J, Zaleski C, Jha S, et al. STAR: ultrafast universal RNA-seq aligner. Bioinformatics 2013;29:15–21.
20. Trapnell C, Williams BA, Pertea G, Mortazavi A, Kwan G, van Baren MJ, et al. Transcript assembly and quantification by RNA-Seq reveals unannotated transcripts and isoform switching during cell differentiation. Nat Biotechnol 2010;28:511–5.
21. Torres-García W, Zheng S, Sivachenko A, Vegesna R, Wang Q, Yao R, et al. PRADA: pipeline for RNA sequencing data analysis. Bioinformatics 2014;30:2224–6.
22. Yoshihara K, Shahmoradgoli M, Martínez E, Vegesna R, Kim H, Torres-Garcia W, et al. Inferring tumour purity and stromal and immune cell admixture from expression data. Nat Commun 2013;4:2612.
23. Brennan CW, Verhaak RGW, McKenna A, Campos B, Noushmehr H, Salama SR, et al. The somatic genomic landscape of glioblastoma. Cell 2013;155:462–77.
24. Goldman M, Craft B, Swatloski T, Ellrott K, Cline M, Diekhans M, et al. The UCSC cancer genomics browser: update 2013. Nucl Acids Res 2013;41:D949–54.
25. Shankar GM, Francis JM, Rinne ML, Ramkissoon SH, Huang FW, Venteicher AS, et al. Rapid intraoperative molecular characterization of glioma. JAMA Oncol 2015;1:662–7.
26. Germer S, Holland MJ, Higuchi R. High-Throughput SNP allele-frequency determination in Pooled DNA Samples by Kinetic PCR. Genome Res 2000;10:258–66.
27. Johnson MP, Haupt LM, Griffiths LR. Locked nucleic acid (LNA) single nucleotide polymorphism (SNP) genotype analysis and validation using real-time PCR. Nucleic Acids Res 2004;32:e55.
28. Latorra D, Campbell K, Wolter A, Hurley JM. Enhanced allele-specific PCR discrimination in SNP genotyping using 3' locked nucleic acid (LNA) primers. Hum Mutat 2003;22:79–85.
29. Bady P, Sciuscio D, Diserens A-C, Bloch J, van den Bent MJ, Marosi C, et al. MGMT methylation analysis of glioblastoma on the Infinium methylation BeadChip identifies two distinct CpG regions associated with gene silencing and outcome, yielding a prediction model for comparisons across datasets, tumor grades, and CIMP-status. Acta Neuropathol 2012;124:547–60.
30. Bell RJA, Rube HT, Kreig A, Mancini A, Fouse SD, Nagarajan RP, et al. The transcription factor GABP selectively binds and activates the mutant TERT promoter in cancer. Science 2015;348:1036–9.
31. Sciuscio D, Diserens A-C, van Dommelen K, Martinet D, Jones G, Janzer R-C, et al. Extent and patterns of MGMT promoter methylation in glioblastoma- and respective glioblastoma-derived spheres. Clin Cancer Res 2011;17:255–66.
32. Hsu C-Y, Ho H-L, Lin S-C, Chang-Chien Y-C, Chen M-H, Hsu SP-C, et al. Prognosis of glioblastoma with faint MGMT methylation-specific PCR product. J Neurooncol 2015;122:179–88.
33. Hambardzumyan D, Gutmann DH, Kettenmann H. The role of microglia and macrophages in glioma maintenance and progression. Nat Neurosci 2015;19:20–7.
34. Meyer M, Reimand J, Lan X, Head R, Zhu X, Kushida M, et al. Single cell-derived clonal analysis of human glioblastoma links functional and genomic heterogeneity. Proc Natl Acad Sci USA 2015;112:851–6.
35. Felsberg J, Thon N, Eigenbrod S, Hentschel B, Sabel MC, Westphal M, et al. Promoter methylation and expression of MGMT and the DNA mismatch repair genes MLH1, MSH2, MSH6 and PMS2 in paired primary and recurrent glioblastomas. Int J Cancer 2011;129:659–70.
36. Bady P, Delorenzi M, Hegi ME. Sensitivity Analysis of the MGMT-STP27 model and impact of genetic and epigenetic context to predict the MGMT methylation status in gliomas and other tumors. J Mol Diagn 2016;18:350–61.
37. Horn S, Figl A, Rachakonda PS, Fischer C, Sucker A, Gast A, et al. TERT promoter mutations in familial and sporadic melanoma. Science 2013;339:959–61.
38. Huang FW, Hodis E, Xu MJ, Kryukov GV, Chin L, Garraway LA. Highly Recurrent TERT promoter mutations in human melanoma. Science 2013;339:957–9.
39. Bell RJA, Rube HT, Xavier-Magalhães A, Costa BM, Mancini A, Song JS, et al. Understanding TERT promoter mutations: a common path to immortality. Mol Cancer Res 2016;14:315–23.
40. Li Y, Zhou Q-L, Sun W, Chandrasekharan P, Cheng HS, Ying Z, et al. Non-canonical NF-κB signalling and ETS1/2 cooperatively drive C250T mutant TERT promoter activation. Nat Cell Biol 2015;17:1327–38.

AACR American Association for Cancer Research

Molecular Cancer Research

Prognostic Relevance of Tumor Purity and Interaction with MGMT Methylation in Glioblastoma

Eva Schulze Heuling, Felix Knab, Josefine Radke, et al.

Mol Cancer Res 2017;15:532-540. Published OnlineFirst February 1, 2017.